Mechanical Design of Instrumentation for Superconducting Lens Validation

Jay Hayman

Table of Contents

Abstract

In support of bringing the PIP-II linac online, robust testing capabilities are required for the validation of superconducting magnetic lenses. To this end, a mechanical design has been outlined for the 3-D measurement of magnetic fields within and outside of these lenses. This report includes design considerations, proposed concepts, and an analytical framework that can be used to specify and optimize components for the mechanical system. Care was taken to leave flexibility for electrical design, which will be a future project.

Introduction

In preparation for the PIP-II expansion of the Fermi accelerator complex, many components will require individual testing and qualification. These tests must be conducted in conditions as close as possible to the working environment to be accurate. While these environments may be reproduced with similar techniques to the actual operating conditions, there may be a lack of testing instrumentation suited for such environments. In this case, the magnetic fields of superconducting focusing lenses must be measured in-situ to ensure that the lenses behave as expected. The lenses in question are intended to be part of the single spoke resonator (SSR) cryomodules in the PIP-II linac. These components are system-critical, as they steer and shape the particle beam to prevent excessive losses and irradiation of the equipment. Each lens (Figure 1) includes several independent electromagnets in different orientations, meaning that the magnetic field can vary in three dimensions. While many tools exist for measuring magnetic fields, they tend to have only one degree of freedom and/or be limited to horizontal test setups in which both ends can be easily accessed [1]. To obtain three degrees of freedom in a top-loaded vertical orientation, a novel device must be designed. This work is concerned with development of the mechanical system, leaving the electrical components and their integration for a later effort.

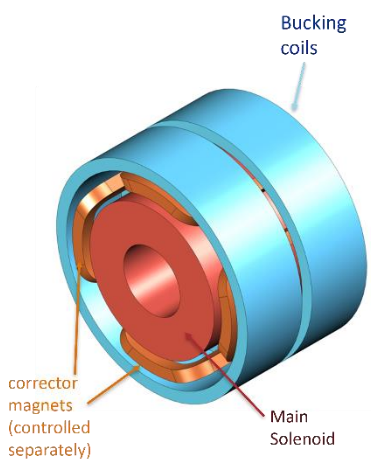

Figure 1: Diagram of a superconducting lens.

Constraints & Considerations

The operating environment for focusing lenses is high vacuum, cooled to liquid helium temperature, and oriented horizontally. For early testing, the lens will be in the vertical orientation, but the other conditions will be replicated in the test environment. This presents a set of challenges. The vacuum conditions require structural reinforcement of any cavities to prevent cave-in. There also must be very tight tolerances on any valve, piston, or other inlet/outlet points to prevent loss of vacuum. If any components within the vacuum output heat, it must be considered that the lack of air means conduction and radiation will dominate heat transfer, with little to no convective cooling. It should also be noted that, because electrical design will occur later, the preferred mechanical system must have a flexible enough design to accommodate wiring, DAQ systems, and digital controls.

Regarding the low temperature, there will be a large thermal gradient from the warm top of the system (~300 Kelvin) to the magnet chilled to 4 K. This means that the system as a whole will experience nonlinear thermal contraction and, since the system will be moving, this contraction will be transient. While it is possible to model this behavior and program controls accordingly, it may be more efficient to actively measure position and use a simple feedback control system. As for thermal interaction between systems, the cryogenic system has a cooling power of 1.5 Watts at temperature. The measurement system will conduct and radiate heat from the outside into the magnet, and this transfer must be kept well below 1.5 W for system compatibility.

As positional accuracy is of high importance, not only in the direction of travel but in the normal plane, some thought must be given to the alignment of the measurement system. First, if possible, the system should be designed such that motion in the plane is resisted. Second, dynamic analysis must be conducted to ensure that any vibrations from motors will not be propagated through the system. Out of plane (axial) motion must be of a magnitude that captures not only the internal field of the lens but the fringe field as well. Although the SSR lens has a specified length of 120 mm, it was requested that the operational stroke be 500 mm, enough to measure 190 mm of fringe field on either side of the lens. Measuring and minimizing the fringe field is crucial because, in addition to blurring the functional boundaries of the lens, stray magnetic fields can interfere with the nearby resonator cavities, impeding the capabilities of the cryomodule as a whole.

Conceptual Design

Multiple system concepts were developed, falling into three major categories: a rigid tower, a bellows with legs, and a bellows with a vertical stage. Before detailing these conceptual groups, there are several commonalities that may be addressed. All systems use a hollow copper alloy (proposed high silicon bronze) rod for positioning. The rod is hollow to achieve a higher flexural strength to mass ratio than a solid rod, decreasing weight and heat capacity. Copper alloys were selected because of copper's weak diamagnetic behavior, making its alloys weakly interacting with the lens's magnetic field, which in turn minimizes systemic interference. Unlike other weak diamagnets (graphite, water, lead), copper alloys are both strong and formable at room temperature, making them ideal for structural applications. To accommodate the variable thermal contraction, all system concepts utilize a pulsed laser time-of-flight distance measurement device. This technology emits a short, focused pulse of photons that reflects off of a surface and is detected by a receiver near the emitter. When it is received, the pulse has traveled twice the distance between the device and the object. By measuring the time step between emission and detection, then multiplying this time step by half the speed of light, the distance to the object can be determined quickly and precisely, even while it is moving. Lastly, all concepts include a probe head (Figure 2) containing multiple Hall probes arranged in the XY plane. Hall probes are common magnetic field measuring devices that detect voltage changes in a circuit due to magnetic deflection of current. Because the current is deflected through a thin foil, Hall probes can only detect field lines normal to the foil. Having probes in multiple positions and orientations allows for three-dimensional field mapping without requiring three-dimensional motion, minimizing potential points of failure. The probe head concept also includes contact rollers, which will keep the probes properly oriented with respect to the axis of the lens.

Figure 2: A rendering of the probe head concept. Slots represent Hall probes in different orientations.

The first concept family, the rigid towers, involves a fully enclosed system in which a reinforced vacuum vessel houses a screw-driven positioning shaft. A motor, mounted within the vacuum, would rotate a threaded collar, which would in turn force a threaded copper alloy shaft to move vertically, carrying a probe head with it. The most usable concept of this family has the motor mounted to the top of the vessel, using the structure as a cooling fin to compensate for the lack of internal air cooling (Figure 3). While this concept delivers on novelty, it presents numerous challenges, among them manufacturability, structural integrity, and the great effort it would take to qualify each custom part.

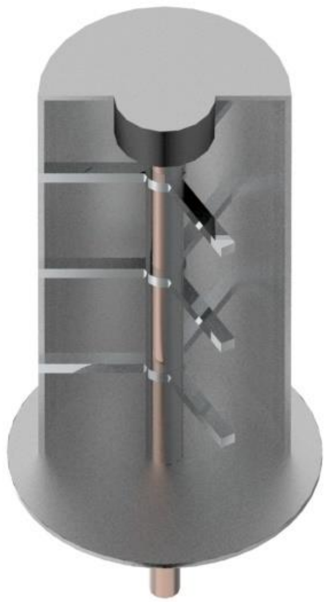

Figure 3: Cutaway of the rigid riser concept, showing internal ribs, copper alloy shaft, and top-mounted motor (black).

To address some of these concerns the bellows with legs family was developed, in which the use of a flexible vacuum bellows allows the motor to sit outside the vacuum and move with the system. The reference concept in Figure 4 uses three vertical legs, along which the motor would drive the system. Since this system would be pulling a plate against the vacuum, rigidity becomes a major concern. The supporting legs would need to be very large in diameter, perhaps prohibitively so, in order to ensure that they do no warp significantly under the stresses of normal use.

Figure 4: Bellows and legs concept, with motor (black) outside vacuum and flexible vacuum bellows shown as translucent.

Finally, a concept was proposed wherein a motorized vertical positioning stage would drive the motion (Figure 5). The system is otherwise identical to the "bellows with legs" concept, with the advantage of having a pre-qualified structure and movement system, as complete stages are available for purchase from several vendors. This design would free up resources for faster optimization of the system as a whole.

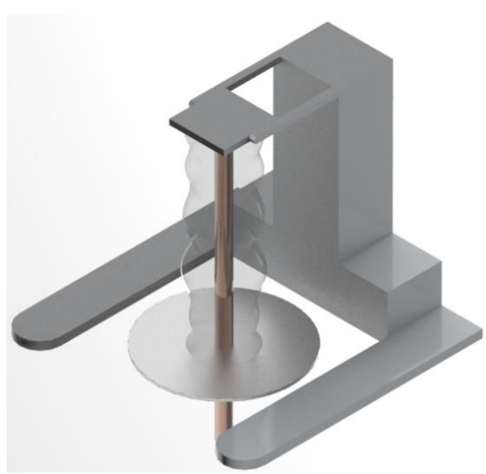

Figure 5: A vertical stage could move a plate fixed to the top of a vacuum bellows.

These three concept families were evaluated with a decision matrix (Figure 6), considering factors such as manufacturability, or the difficulty a machinist or other manufacturer may experience in making parts to tolerance; calibration requirements, related to the number and importance of custom components and subassemblies that would need to be certified and calibrated; and upgradability, looking forwards to the potential to change parts for better ones in the future. After weighting the categories and scoring each concept, the "bellows and stage" concept was selected as the preferred design.

Criterion	Weight	Rigid Tower	Bellows & Legs	Bellows & Stage
Manufacturability	10	1	2	3
Materials Cost	10	2	3	1
Labor Cost	10	1	2	3
Calibration	15	1	1	3
Maintenance	5	1	3	3
Service & Upgrades	15	1	2	3
Reliability	10	3	2	3
Footprint	15	1	2	3
Novelty/Fun	15	2	3	1
Weighted Total:	**105**	**50**	**75**	**88.33333333**

Figure 6: The decision matrix used to select the preferred concept, including total scores.

Analysis Methodology

```
% Japheth Hayman
% August 8, 2022
% Analysis of magnet test stand components
% C65500 silicon bronze tubes
% Atlas Metal stock dimensions, matweb properties
clear; close all; clc

%% Input Parameters
% Shaft
E=105e9; %modulus of elasticity, N/m^2
L=1; %free length, m
rho=8.53e3; %density, kg/m^3
c=0.380; %specific heat, kJ/kg-K
eps=0.044; %coating/wrap emissivity - aluminized mylar [Domen 1991]
do=[1 0.75 0.5]*25.4/1000; %outer diameter, m
di=[0.75 0.562 0.344]*25.4/1000; %inner diameter, m
% di=zeros(1,length(do)); %solid shaft

% Bellows
% Wb=; %weight, N
IdB=4*25.4; %internal diameter, mm

%% Natural Frequencies
f=@(x) cos(x).*cosh(x)+1; %frequency formula for cantilever beam [Whitney 1999]
n=3; %number of zeros to find
x=zeros(1,n);
for i=1:n
    x(i)=fzero(f,pi*i-pi/2); %starting at pi/2 and increasing by pi
```

Figure 7: Beginning of the MATLAB analysis script, including input variables and placeholders for future considerations.

While concepts for movement and external structure were being developed, analysis was conducted on the copper alloy rod that acts as a critical member in all designs. This analysis was carried out using a MATLAB script (Figure 7) in which a user can edit rod geometry and material properties, and the script outputs a table of static, dynamic, and thermal properties of the rod. Test calculations were done with C65500 high silicon bronze [2] using three stock tube sizes from a vendor [3] and 1-meter free length. The key static property is flexural stiffness, which indicates the restoring force when the free end is displaced from center. This is calculated by inverting the equation for end deflection of a cantilever beam, yielding:

$$K = \frac{3EI}{L^3},$$ [Eq. 1]

where K is the flexural stiffness in N/m, E is the material's elastic modulus in Pascals, I is the section's area moment of inertia in m^4, and L is the beam length in meters. The inverse of flexural stiffness indicates force required to bend the rod, which is significant for probe head material selection. It must be strong enough to keep the rod centered, even if thermal contraction tends to bend it. As mentioned, the key dynamic behavior is vibration, especially the natural frequency of the rod. For this, it is once again modeled as a cantilever beam, ignoring the opposition the probe head may provide. This consideration is dropped so that the head can be designed only for static forces, and dynamic forces can be addressed by careful design of the rest of the system. Free oscillation modes of a general cantilever beam are first calculated using

$$\cos\alpha \cosh\alpha = -1,$$ [Eq. 2]

with dimensionless frequency parameter α, then converted to natural frequencies of specific rods using

$$\left(\frac{\alpha}{L}\right)^4 = \frac{\omega^2\lambda}{EI},$$ [Eq. 3]

for natural frequency ω in rad/s and linear mass density λ in kg/m [4]. It was determined that, for a high aspect ratio rod, thermoelastic damping will be negligible and is therefore excluded [5]. Since Equation 2 is transcendental, it can be used to find many harmonics of increasing frequency. If the driving motor spins at a harmonic of the rod, its vibrations may be amplified through the system, causing detrimental oscillations. The motor and rod must then be selected as a pair so as to prevent such resonance. Finally, the ever-crucial thermal behaviors of the system include total heat transfer and maximum dissipation rate. Total heat transfer is calculated simply by taking the heat capacity of the rod (from mass and specific heat) and multiplying by the maximum change in temperature, 300 K to 4 K. This, of course, assumes that the entire rod is cooled to the temperature of the lens, which is most likely a very large over-estimate. Maximum dissipation rate is determined as the grey body radiative heat transfer between the rod at room temperature, most likely wrapped in an insulator, and the SS 316L bore of the main solenoid, modeled as infinite concentric cylinders:

$$q = \frac{\sigma A_i \left(T_i^4 - T_o^4\right)}{\frac{1}{\epsilon_i} + \frac{1-\epsilon_o}{\epsilon_0}\left(\frac{r_i}{r_o}\right)} \quad \text{[Eq. 4]}$$

where q is the net heat exchange in Watts, the Stefan-Boltzmann constant $\sigma = 5.670 \times 10^{-8}\ W/m^2 \cdot K^4$, surface area A in m^2, temperature T in Kelvin, dimensionless emissivity ϵ, radius r in meters, and inner and outer cylinders denoted with the subscripts i and o, respectively. For the sample calculation, the rod is wrapped in aluminized mylar, which has very low emissivity [6]. Without wrapping, the heat transfer for some rods may be too high for the cooling system to accommodate. Conduction was neglected in this model because the rollers on the probe head have very small contact areas, and may be removed from the design altogether if a rod is selected such that gravity can maintain alignment without contact supports.

Results & Recommendations

Figure 8 shows sample output from the analysis script. Worth note is the first harmonic of Rod 3, the smallest size tested. Its natural frequency of 15.1 Hz corresponds to a motor speed of about 900 rpm. While this is not likely to be a concern for a high-torque electric motor, smaller rods may have harmonics within the operating speed of some stage motors. Also notable is the heat output, which for all three rods is on the order of 10% of the available cooling power. The final design decision may well be a matter of minimizing heat output without crossing a certain minimum resonance frequency.

	Rod 1	Rod 2	Rod 3
Outer Diameter (mm)	25.4	19.05	12.7
Inner Diameter (mm)	19.05	14.275	8.7376
Flexural Stiffness (kN/mm)	0.017598	0.0055774	0.0012485
First Harmonic (Hz)	31.168	23.368	15.133
Second Harmonic (Hz)	195.32	146.45	94.835
Third Harmonic (Hz)	546.91	410.05	265.54
Thermal Energy (J)	212.7	119.91	64.01
Heat Output (W)	0.17854	0.13654	0.092859

Figure 8: Sample output from the analysis script.

Future analysis efforts should include vibration modeling with the mass and constraints of the probe head, radiative heat transfer modeling that considers edge effects and transient behavior, and conductive heat transfer from rollers. The hot spots that these rollers may create on the inner solenoid are especially important considerations for ensuring proper lens performance during testing.

Acknowledgements

This author would like first and foremost to thank Cristian Boffo for his expert supervision, Darren Crawford and Karie Badgley for their support and advice, and both Fermilab and the National GEM Consortium for their support and funding. Also deserving of praise are Dr. Judy Schneider and Mr. Brody Montgomery, both of whom were invaluable discussion partners in the early ideation phase of this project.

Works Cited

[1] N. Glamann, D. Saez de Jauregui and S. Casalbuoni, *Magnetic Measurement Systems for Superconducting Undulators*, Karlsruhe Institute of Technology, 2021.

[2] "MatWeb - Material Property Data," [Online]. Available: http://matweb.com. [Accessed 28 June 2022].

[3] Atlas Metal Sales, "Silicon Bronze Round Tube," 2022. [Online]. Available: https://atlasmetal.com/silicon-bronze-round-tube.php. [Accessed 12 July 2022].

[4] S. Whitney, "Vibrations of Cantilever Beams: Deflection, Frequency, and Research Uses," 23 April 1999. [Online]. Available: http://emweb.unl.edu/Mechanics-Pages/Scott-Whitney/325hweb/Beams.htm. [Accessed 12 July 2022].

[5] F. M. Foong, T. C. Ket and D. Yurchenko, "On mechanical damping of cantilever beam-based electromagnetic resonators," *Elsevier BV*, March 2019.

[6] S. R. Domen, "Emissivity of aluminized mylar," *International Journal of Radiation Applications & Instrumentation*, vol. 37, no. 2, pp. 199-201, 1991.